Title: Catalytic Behaviour of Mesoporous Metal Phosphates in the Gas-phase Glycerol Transformation

Author: S. Lopez-Pedrajas R. Estevez R. Navarro D. Luna F.M. Bautista

PII: S1381-1169(16)30186-8
DOI: http://dx.doi.org/doi:10.1016/j.molcata.2016.05.015
Reference: MOLCAA 9890

To appear in: *Journal of Molecular Catalysis A: Chemical*

Received date: 25-2-2016
Revised date: 10-5-2016
Accepted date: 13-5-2016

Please cite this article as: S.Lopez-Pedrajas, R.Estevez, R.Navarro, D.Luna, F.M.Bautista, Catalytic Behaviour of Mesoporous Metal Phosphates in the Gas-phase Glycerol Transformation, Journal of Molecular Catalysis A: Chemical http://dx.doi.org/10.1016/j.molcata.2016.05.015

Highlights

- ✓ Simple (M= Al, Fe, Co, Mn) and binary (Al/M; M=Fe,V,Ca) metal phosphates presented good stability
- ✓ Acidity, redox sites and morphology of metal phosphates are influential in acrolein formation
- ✓ Amorphous Fe and Al phosphates were more active than those with a high crystalline character (Co, Mn, Cu)
- ✓ Al-V phosphate composed of partially-crystallized $AlPO_4$ and β-$VOPO_4$, showed the highest activity in the acrolein formation

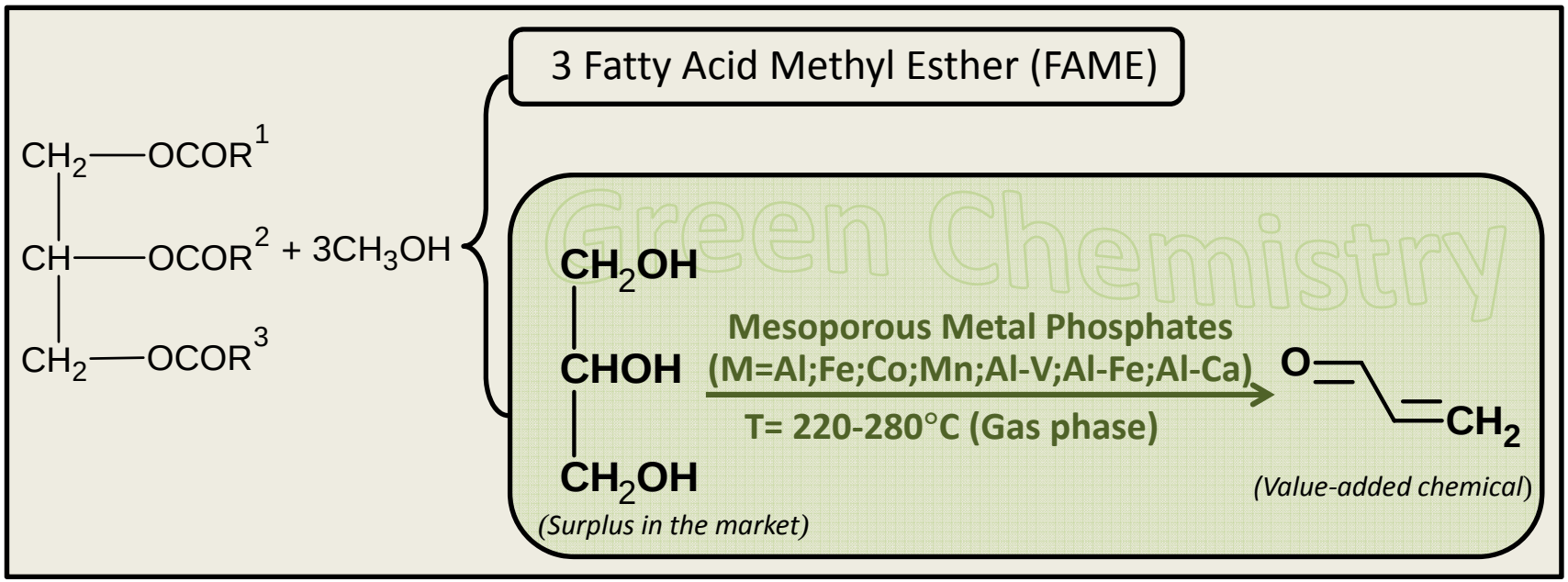

Graphical abstract

Catalytic Behaviour of Mesoporous Metal Phosphates in the Gas-phase Glycerol Transformation

S. Lopez-Pedrajas*, R. Estevez, R. Navarro, D. Luna, F.M.Bautista**

*Departamento Química Orgánica, Instituto de Química Fina y Nanoquímica, Universidad de Córdoba, Campus de Excelencia Internacional Agroalimentario, CeiA3. Edificio Marie Curie, E-14014 Córdoba, Spain, e-mail: *q52lopes@uco.es, **fmbautista@uco.es*

Keywords: glycerol transformation; acrolein formation; acrolein formation activation energy; amorphous metal phosphate; amorphous aluminium phosphate; pyridine TPD

All correspondence concerning this manuscript should be addressed to:

Dña. Susana López Pedrajas — Prof. Dra. Felipa Mª Bautista

Departamento Química Orgánica — Departamento Química Orgánica

Universidad de Córdoba — Universidad de Córdoba

Campus de Rabanales, Edificio Marie Curie, E-14014-Córdoba, España

Fax: (+34)957212066

e-mail: q52lopes@uco.es — fmbautista@uco.es

Abstract

The catalytic behaviour of mesoporous simple (M= Al, Fe, Co, Mn) and binary (Al/M; M=Fe,V,Ca; molar ratio Al/Fe=50; Al/V=2; Al/Ca=1) metal phosphates, synthesized by an economical gelation method, in the gas-phase glycerol reaction at temperatures between 220ºC and 280ºC, has been investigated. The morphology, textural properties and the acidity by pyridine TPD, of the phosphates were also determined. The activity of the phosphates in the formation of the main reaction product (acrolein) depended not only on their acidity (mainly acid sites of weak-medium strength) but also on the redox sites and morphology exhibited. Thus, the aluminum-vanadium phosphate showed the highest value of yield to acrolein, 62% (equivalent to a productivity of 0.88 $\frac{g_{ACR}}{g_{cat} \cdot h}$) at 280ºC, whereas the amorphous $FePO_4$ and $AlPO_4$ were appreciably more active than the rest of the simple phosphates, exhibiting a high crystalline character. The apparent activation energy values obtained for the acrolein formation ranged between 18 and 91 kJ/mol. Based on the identified products in this study, some possible reactions involved in the glycerol transformation have been suggested.

1. Introduction

Nowadays, the demand for energy is almost exclusively covered by basic fossil materials (crude oil, natural gas, coal), but sooner or later we are going to run out of these materials. Also, these non-renewable fossil resources have adverse environmental impacts, such as the formation of large amounts of CO_2 in the atmosphere and its negative influence on global warming (the greenhouse effect). Due to this situation, the use of renewable resources, such as biomass, as feedstock for the production of fuels and chemicals, has become an increasingly important focus in energy-related catalysis. Glycerol is one of these renewable resources that is mainly obtained as a sub-product during the biodiesel production. In fact, for every 1000 kg of biodiesel produced, 100 kg of glycerol are obtained.

The total biodiesel production in developing countries is estimated to increase to 14 billion litres by 2022 [1], but the current application of glycerol remains practically invariable. Therefore, a drastic surplus of glycerol in the chemical markets is expected.

Glycerol is non-toxic, biodegradable and a potential starting material for numerous value-added chemicals which can be obtained from reactions such as dehydration, oxidation, etherification, esterification, reforming, etc, mainly, on heterogeneous catalysts [2-5]. These transformations would increase the utility of glycerol, resulting in a reduction in the cost of biodiesel production [2].

Acrolein is one of these value-added chemical molecules, which is employed as an important and versatile intermedium in the chemical industry, mainly, in the production of acrylic acid esters and DL-methionine.

Currently, acrolein is mainly produced by catalytic oxidation of propylene (petroleum derived) in the gas phase on a Bi/Mo-mixed oxide with high values of

conversion and selectivity. Therefore, the double dehydration of glycerol would offer a promising ecofriendly alternative to the current oil-dependent commercial process.

The dehydration of glycerol yielding acrolein as in the dehydration reaction of alcohols requires an acid catalyst. Thus, this reaction has been tested in homogeneous medium using acids such as sulfonic acid. Indeed, it has been studied in a heterogeneous medium, in both liquid and gas phases, with various solid acids such as phosphates, sulfates and oxides of metal; supported heteropolyacids and zeolites, in the absence or in the presence of oxygen, as has been reported in recent reviews [6, 7].

One of the most studied catalysts for the dehydration of glycerol in gas phase is the system WO_3/ZrO_2, whose activity in the production of acrolein depends on the content of WO_3. Thus, Dubois et al. [8] with a content of 9.3 wt% reported a yield to acrolein (Y_{ACR}) of 73.5% at 300ºC, whereas Chai et al. [9] obtained 65% at 315ºC with a content of 15 wt%. Lauriol-Garbey et al. [10] after doping of the catalytic system with SiO_2, improved the selectivity to acrolein at 300ºC from 70% to 78% at nearly total glycerol conversion, and also its stability. Zeolites and heteropolyacids have also been widely employed due to their strong Brönsted acid sites. The HZSM-5 is one of the most studied molecular sieves in this reaction [9, 11-13]. Thus, Kim et al. [11] achieved a Y_{ACR} of 48% on zeolite with SiO_2/Al_2O_3=150 ratio and Wang et al. [13] improved the Y_{ACR} from 36% to 54% by adding Al to this zeolite. Likewise, a better performance of the heteropolyacids was obtained by using modifiers, as reported by Alhanash [14], which exhibited a higher stability than the unmodified heteropolyacid, maintaining a high Y_{ACR} (76%), by doping with 0.5 wt% of Pd.

As far as the phosphates are concerned, Suprun et al. [15] prepared systems based on Al_2O_3 or TiO_2 modified with H_3PO_4 by impregnation, which exhibited higher activity but less selectivity towards acrolein (Y_{ACR}=42%) than the microporous

silicoaluminophosphates (Y_{ACR}=55%). By introducing different transition metal oxides (W, Mo, Cu, Fe, V, Cr, Ce) in the PO_4/Al_2O_3, a higher Y_{ACR} (65%) was attained [16]. Deleplanque et al. [17] obtained 92% of acrolein with a well-crystallised $FePO_4$ prepared by hydrothermal synthesis. Likewise, Wang et al. [18] obtained Y_{ACR} of 66% with vanadium phosphate oxide, but in the presence of molecular oxygen, in order to reduce the deactivation of the catalyst. However, vanadium phosphorous oxides with different P/V ratios were deactivated even with the presence of air, as reported by Rajan et al. [19].

Despite the fact that this reaction has been extensively studied, discrepancies still exist about the type of acid sites (nature and strength) that catalyse this reaction. Some studies [9, 14] indicated a strong influence of the Brönsted acid sites in the production of acrolein, although a cooperation between the Brönsted and Lewis acid sites has also been reported [13]. Furthermore, the strength of the acid sites is a determining factor to be taken into account, given that the stronger sites, in particular, promote the coke formation and therefore causing a rapid deactivation of the catalysts. However, apart from the acid properties of the catalysts, other factors must be considered in order to explain the results found in the literature. Such factors are the external surface area [12, 15], the size of the pores [9, 12, 15], the structure [17] and the tolerance to water [11, 12, 20] among others.

On this basis and in the context of a research aimed at the revalorization of glycerol, we studied the production of acrolein in gas phase employing simple and binary metal phosphates based on aluminium phosphate, synthetized by a simple and economical sol-gel method. The morphology, porosity and the acid properties of aluminium phosphate depend on the synthesis parameters (starting aluminium salt,

gelling agent) [21, 22] and the presence of other metals [23-25]. The relationship between their acid properties and the catalytic behaviour of the phosphates in the dehydration of different alcohols has also been demonstrated [24-27]. Moreover, not only the acidity, but also the porosity were responsible for the highest activity of amorphous aluminum phosphates in comparison with commercial zeolites (H-ZSM-5 and HY) in the production of acrolein from glycerol but in liquid phase, as we have recently reported [28].

In the present paper, in addition to aluminium phosphate we have studied phosphates of Fe, Co, Mn and Cu, all of them with variable cation valency (redox sites) because our final objective is the transformation of glycerol in acrylic acid in one step. Furthermore, we have studied several binary Al/M (M=Fe, V, Ca) phosphates in order to know the influence of a second metal in the catalytic behaviour of aluminium phosphate in the glycerol transformation. As far as we known, binary phosphates such as those employed in this research, have not been investigated before for glycerol transformation. The morphology, textural properties and acidity by Temperature Programmed Desorption of pyridine (Py-TPD) of the phosphates were also evaluated.

2. Experimental

2.1 Catalyst preparation

The solids were prepared by a sol-gel method as previously reported [23, 25, 26]. Thus, the metal (Mn, Co, Al, Fe) phosphates were synthesized from aqueous solutions of chlorides ($MnCl_2.4H_2O$, 99 wt%, Probus; $AlCl_3.6H_2O$, 99 wt%, Fluka) or nitrates ($Co(NO_3)_2.6H_2O$, 99 wt%, Merck; $Fe(NO_3)_3.9H_2O$, 98 wt%, Probus) of the corresponding metal and H_3PO_4 (85 wt%, Panreac) by precipitation with aqueous ammonia (25 wt%, Panreac) and stirring at 0ºC. The precipitation was allowed to stand

at room temperature. The pH value at the precipitation 'end point' was between 6 and 7. After filtration the solid was washed with 2-propanol (99.5 wt%, Panreac), dried at 120ºC for 24 h and calcined in air for 3 h. The metal phosphates are denoted by the corresponding theoretical formula and a number indicating the calcination temperature, generally 450ºC. Copper pyrophosphate ($Cu_2P_2O_7 \cdot xH_2O$), a commercial solid, acquired from Probus, was employed after calcination at 450ºC.

The binary phosphates of Al and M (M=Fe, Ca and V) following the same method as indicated for simple phosphates, were prepared from an aqueous solution of the appropriate amounts of $AlCl_3.6H_2O$ and the corresponding salt, $Fe(NO_3)_3.9H_2O$; $CaCl_2.2H_2O$ (99 wt%, Sigma-Aldrich) and vanadyl oxalate, respectively, and H_3PO_4. The vanadyl oxalate was prepared from NH_4VO_3 (99 wt%, Aldrich) reduced with oxalic acid (99.5 wt%, Merck). The pH value at the precipitation 'end point' was 6.7 for Al-Fe [23]; 6.1 for Al-Ca [25] and 4 for Al-V [24] and the molar ratio P/Al+M = 1; 0.8 and 0.7, respectively. After the filtration and drying processes, the solids were calcined in air at 450ºC. These systems will be denoted as AlMPO(x)450, where x indicates the Al/M theorical molar ratio and 450 the calcination temperature.

For comparative purposes, a system ($1Fe/AlPO_4$-450) obtained by impregnation of an aluminium phosphate calcined at 350ºC with a solution of $Fe(NO_3)_3.9H_2O$ in methanol, was also employed [23]. Its calcination temperature (450ºC) and iron content (1wt%) were the same as those of the aforementioned co-precipitated system.

All the solids were screened at <0.149 mm to avoid internal diffusion limitations in the reactions.

2.2. Characterization of catalysts

X-ray diffraction (XRD) patterns were obtained using Ni-filtered Cu K_α radiation (λ = 1.5406 Å). Finely ground samples were scanned at a speed of 2º/min (2º ≤ 2θ ≤ 80º) using a Siemens D-500 diffractometer (40 kV, 30 mA).

The textural properties were determined from the adsorption-desorption isotherms of nitrogen, at the temperature of liquid nitrogen (77 K), using a Micromeritics ASAP 2000 apparatus. Previously, the samples were degassed to 0.1 Pa. BET surface areas were determined applying equation at relative pressures in the range p/p_0=0.05-0.30, assuming a cross-sectional area of 0.162 nm^2 for the nitrogen molecule. The pore size distribution was calculated using the method of Barrett, Joyner and Halenda (BJH) assuming a cylindrical pore model.

The Py-TPD experiments were carried out in a versatile apparatus from PID Eng&Tech with a thermal conductivity detector (TCD) with helium as the carrier gas. Before the adsorption experiments were started, the catalyst (30 mg) was pretreated in situ from room temperature to 400ºC (rate of 20ºC/min). After the catalyst pretreatment, saturation of the sample with pyridine was carried out at 50ºC during 30 min, thereafter, physisorbed pyridine was desorbed at 50ºC during 60 min. Then, the measurements were performed in the range 50-450ºC with a heating rate of 10ºC/min to remove the chemisorbed pyridine.

The coke determination was carried out by Termogravimetric analyses (TGA) using a Cahn 2000 thermobalance in the presence of static air with a 20 mg sample. The heating rate was 10ºC/min (temperature range: 30-1000ºC).

2.3. Glycerol transformation

The glycerol transformation was carried out in a continuous-flow fixed-bed reactor under atmospheric pressure, as previously described [23]. The reactor was made

of stainless-steel tubing (7 mm internal diameter and 190 mm long), placed in a tubular electric furnace. The temperature was monitored by a thermocouple located in the catalyst bed. The analysis of the feed and reaction products was carried out on-line using a multicolumn gas chromatograph (GC) equipped with both flame ionization (FID) and thermal conductivity (TCD) detectors in parallel. The compounds were separated in a capillary column, DB-1 (100% methylpolysiloxane, 60 m x 0,25 mm x 0,25 μm).

The catalyst (100 mg) was pretreated at the reaction temperature during 2 h in a N_2 flow (75 mL/min). A 36 wt% glycerol (99.5%, Sigma-Aldrich) aqueous solution was fed at 0.6 mL/h (0.69 μmol/s of glycerol). In general, each catalytic test was conducted at least for 3 h at different temperatures (220ºC, 250ºC and 280ºC). The reaction products were identified by chromatographic patterns and/or a gas chromatograph-mass spectrometer (GC-MS) (VARIAN CP 3800, QUADRUPOLE MS 1200) also equipped with a capillary column DB-1. A blank test showed the absence of homogeneous reactions and the reactor inactivity in the absence of a catalyst.

The glycerol conversion (X_{Gly}) was calculated from $X_{Gly}= (mol_{Gly,in}-mol_{Gly,out})\cdot 100/mol_{Gly,in,}$ whereas the selectivity (S_i) and the yield (Y_i) to product i were expressed as mol% on a C atom basis. Carbon balance (mol%) was calculated by summing up the amount of unreacted glycerol and the total quantities of identified products.

The values of acrolein formation rate (r_{ACR}) were obtained from the equation: $r_{ACR}= Y_{ACR}\cdot F_{Gly}/100\cdot w$, where w is the catalyst weight (g), and F_{Gly} is the feed rate of glycerol (mol/s).

3. Results and Discussion

3.1. Characterization of the solids

Figure 1 shows the XRD pattern of the different solids. As can be seen, the $AlPO_4$450 only showed a very broad hump in the range 2θ between 15-40º, a characteristic of the amorphous metal phosphates [21]. The $AlPO_4$550 and the $FePO_4$450 also exhibited an amorphous character with diffractograms similar to that of $AlPO_4$450. On the contrary, the $Co_3(PO_4)_2$450 and the $Mn_3(PO_4)_2$450 showed certain crystalline character, with reflections attributed to monoclinic $Mn_2P_2O_7$ (JCPDS 29-0891) and $Co_2P_2O_7$ (JCPDS 34-1378), respectively. The commercial $Cu_2P_2O_7$450 pattern was in accordance with its structure, a copper pyrophosphate (JCPDS 44-0182).

As far as the binary systems are concerned, the addition of a small amount of Fe to the precipitation medium of $AlPO_4$ did not change the amorphous character of the aluminium phosphate [23], whereas the presence of V promoted its crystallization. Thus, the pattern of the AlVPO(2)450 showed reflections attributed to aluminium phosphate, partially crystallized in α-cristobalite form (JCPDS 11-500) and to a specific phase of vanadium as β-$VOPO_4$, (JCPDS 27-948) [24]. In the case of AlCaPO(1)450, the results were not so clear with a pattern exhibiting peaks assigned to CaP_2O_6 (JCPDS 15-0231) and a broad hump in the same range as the amorphous $AlPO_4$450.

(Figure 1, near here)

According to the textural analysis, the nitrogen isotherms obtained for all the catalysts studied were type IV of the Brunauer, Deming, Deming y Teller (BDDT) classification, exhibiting H1 hysteresis loops that indicate mesoporous solids. Furthemore, t-plots (using Harkins-Jura correlation) from the adsorption branch of the isotherm, showed the absence of microporisity. The values of surface area, S_{BET}, of pore

volume, V_P, and of mean pore diameter, d_P, obtained, as well as the pore size distributions are compiled in Table 1. These results showed that when the crystalline character of the solids increased, the S_{BET} and V_p values decreased and the d_p increased. Thus, the S_{BET} and V_p values of the $Mn_3(PO_4)_2$450, $Co_3(PO_4)_2$450 and $Cu_2P_2O_7$450 were appreciably lower (and the d_p higher) than those of the $AlPO_4$, regardless of its calcination temperature, whereas this fact is less noticeable in the amorphous $FePO_4$450. In fact, such crystalline solids exhibited a higher percentage of macropores (>500 Å) than mesopores (500-20 Å). Likewise, the binary systems containing V or Ca showed significant changes in their textual properties in comparison with $AlPO_4$, whereas those corresponding to binary phosphates containing Fe were hardly modified, Table 1.

(Table 1 and Figure 2, near here)

The results from Py-TPD, Figure 2, indicated again the differences that exist between the crystalline phosphates and the amorphous ones. Thus, $Mn_3(PO_4)_2$450, $Co_3(PO_4)_2$450 and $Cu_2P_2O_7$450 adsorbed a very low amount of pyridine, Table 1, according to their almost plane Py-TPD profiles, whereas the profiles of the rest of the solids were similar, showing a maximum in intensity between 100ºC and 200ºC. Furthermore, with the exception of the AlCaPO(1)450 profile, the other ones never reached the baseline.

The acid sites were classified on the basis of their strengths, according to the following criteria in the pyridine desorption temperatures: weak (80-200ºC), medium (200-300ºC) and strong (> 300ºC). The results are also compiled in Table 1. In general, the solids with a higher S_{BET} presented a higher value of acidity. Thus, the crystalline simple phosphates exhibited a very low acidity (4 μmol/g). The $AlPO_4$, regardless of the

calcination temperature, showed a value of acidity around 140 μmol/g and a density of acid sites of 0.6-0.7 μmol/m^2, the weak sites predominating (around 70%). These types of sites were also predominant in the $FePO_4$, although this phosphate exhibited a higher percentage of strong acid sites than the $AlPO_4$. Furthermore, it is noticeable that the $FePO_4$ is the solid with the highest density of acid sites. Consequently, the density of acid sites of the Fe-Al phosphates was intermediate to that of the corresponding simple phosphates. Likewise, the other two binary phosphates showed a higher density of acid sites than $AlPO_4$, especially the V-Al phosphate that additionally showed the highest value of density of strong acid sites (0.32 μmol/m^2). Therefore, the coordination of a metal exhibiting redox properties (Fe and V) with PO_4 and/or AlO_4 tetrahedral of aluminium phosphate generated new strong acid sites, which were not generated when the metal did not have redox properties such as Ca.

3.2. Glycerol transformation

3.2.1 Products of reaction

In addition to acrolein, which was the main product from glycerol on all the solids studied, other products were also obtained, as can be seen in Scheme 1. They were products of intramolecular glycerol dehydration; acrolein (ACR); hydroxyacetone (HA) and glycidol (GD) and of intermolecular dehydration, diglycerol (DGly). Products of glycerol acetalization with formaldehyde, glycerol formal (GF), which is a mixture of 1,3-dioxan-5-ol and 4-hydroxymethyl-1,3-dioxolane. Products of degradation and/or oxidation of glycerol as hydroxyacetic acid or glycolic acid (GA) and its derivate, ethyl glycolate (EG), were also obtained. Additionally, it should be noted that in the condensed effluent at the end of some catalytic runs, formic acid was also identified by

MS. However, it was not detected by TCD in any of the simple analyse. Likewise, CO_2 and CO were not detected.

(Scheme 1, near here)

3.2.2. Influence of the reaction parameters

A general characteristic of all the catalysts studied was their high stability or resistance to deactivation in the glycerol transformation under the present experimental conditions. This property is very important, taking into account that the deactivation of the catalysts is one of the problems described for this reaction as indicated in the Introduction [11, 12, 14, 15, 19, 20, 29]. Thus, for all the catalysts, the steady state was reached at 2-3h of time on stream and the conversion values did not undergo changes after around 14 h of operation, as shown in Figure 3 for $Mn_3(PO_4)_2$450, $AlPO_4$450 and 1Fe/$AlPO_4$-450. Furthermore, it is worth mentioning that the most active catalysts showed the highest differences between the values of conversion at the beginning of the reaction (i.e. at 6 min on stream) and in the steady state, as happened for 1Fe/$AlPO_4$-450 in Figure 3. This fact could be explained due to the coke formation that would take place preferably at the beginning of the reaction and would be accentuated as the reaction temperature rises [28]. Thus, after the catalytic test, such catalysts became slightly black and the thermogravimetric analysis confirmed the formation of coke (<6 wt%).

The influence of contact time (w/F_{Gly}) and reaction temperature on the glycerol conversion and selectivity (or yield) to reaction products, has also been studied. The effect of the contact time on the catalytic activity was examined by changing the weight of the catalyst, as can be seen in Figure 4. When the contact time was double the conversion increased from 10% to 23%, the selectivity to acrolein remained constant and the selectivity to the main by-products, hydroxyacetone and glycerol formal,

decreased at the expense of the diglycerol formation. Hence, an increase in the weight of the catalyst especially favoured the formation of acrolein, whose formation was also favoured by the temperature as well as the formation of all the by-products, Figure 5. The same tendency has been reported by the formation of acrolein and of hydroxyacetone, which is the main by-product described [11, 14-16, 30, 31].

(Figures 3, 4 and 5, near here)

3.*2.3. Catalytic behaviour of all the phosphates studied*

The values of glycerol conversion and selectivity to acrolein obtained with all the catalysts at the three studied reaction temperatures are shown in Figure 6. As expected, the conversion values of the Al and Fe simple phosphates were appreciably higher than those of Mn, Co and Cu phosphates, especially at temperatures superior to 220ºC. Thus, values of 74% and 78% were attained at 280ºC with $AlPO_4$450 and $FePO_4$450, respectively, whereas a 19% value was obtained with $Co_3(PO_4)_2$450, which was higher than those corresponding to Mn and Cu phosphates.

However, the highest values of conversion, practically 100%, were obtained at the same temperature with the binary Al-V phosphate and the 1Fe/$AlPO_4$-450 supported system. Conversely, the presence of Ca did not promote the activity of $AlPO_4$, the Al-Ca phosphate showing a maximum conversion value of only 23%. Nevertheless, this was one of the phosphates exhibiting a high value of acrolein selectivity at the three studied temperatures (around 80% at 220ºC), as can be seen in Figure 6.

(Figure 6, near hear)

In general, an increase in the conversion value (which increased when the temperature increased) resulted in a decrease in the acrolein selectivity value, especially with the more active phosphates. Thus, for instance the acrolein selectivity decreased

from 90% (at 220ºC) to 54% (at 280ºC) on $FePO_4$. These results agree with those obtained by Kongpatpanich et al. [32], and disagree with those reported by Kim [11] and Carriço [20], who observed an increase in the selectivity values when the temperature increased.

However, in all the cases the yield to acrolein is favoured by the temperature in clear accordance with the results in Figure 5. At 280ºC the capacity of the solids to produce acrolein followed this order: AlVPO(2)450 > 1Fe/$AlPO_4$-450 > $FePO_4$450 > AlFePO(50)450 > $AlPO_4$450 > $AlPO_4$550 > AlCaPO(1)450 > $Co_3(PO_4)_2$450 > $Mn_3(PO_4)_2$450 > $Cu_2P_2O_7$450. In fact, a yield of 62% was achieved with AlVPO(2)450, that is comparable to those reported employing phosphates as catalysts. Thus, Suprun et al. [16] obtained 65% on WO_x-PO_4/Al_2O_3 at 265ºC and Wang et al. [18] 66% of acrolein on VPO at 300ºC, but in the presence of oxygen, whereas Deleplanque et al. [17] attained a significantly higher Y_{ACR} (92.1%) at 280ºC with a well-crystallised iron phosphate prepared by hydrothermal synthesis. However, the acrolein productivity ($\frac{g_{ACR}}{g_{cat} \cdot h}$) attained with this catalyst was inferior to that obtained with AlVPO(2)450, as can be seen in Table 2, in which the highest values of acrolein productivity obtained in the present study are shown, along with others reported in the literature for several phosphates. The productivity obtained here (0.46 $\frac{g_{ACR}}{g_{cat} \cdot h}$) with $AlPO_4$450 was appreciably superior (almost seven times) to that which we previously reported in liquid phase (0.07 $\frac{g_{ACR}}{g_{cat} \cdot h}$) [28]. In fact, in this previous research the highest productivity was attained on $AlPO_4$ but calcined at 650ºC (Table 2).

(Table 2, near here)

With regard to the secondary products, their formation also depended on the catalyst, as can be seen in Figure 7, in which the values of selectivity to by-products obtained at 280ºC are collected. Thus, the catalysts with the highest capacity to produce acrolein, in addition to generating coke at the beginning of the reaction, also generated some compounds in the steady state, which were not detected and whose yields were calculated from the carbon-balance. Such compounds are denoted by "others" in Figure 7 and should be responsible for some obstruction of the reaction system lines during the experiments, despite such lines being at a temperature of 200ºC. For $FePO_4$; $1Fe/AlPO_4$ and AlVPO, catalysts the selectivity values to these compounds were superior to the rest of the by-products, attaining a value of around 40% for $1Fe/AlPO_4$. In this sense, appreciable amounts of unidentified compounds, which could be the result of the polymerization of the glycerol or of some products of the reaction, have been reported regardless of the type of catalyst (oxides, phosphates or zeolites) [9, 11, 12, 15]. As can also be seen in Figure 7, the main by-product (around 20%) obtained with the Al phosphates and with the less active phosphates (Cu and Mn) were hydroxyacetone and the dimer of the glycerol, respectively. The values of selectivity to the rest of by-products hardly attained 10%, with the exception of glycolic acid, which attained a value of 23% with $AlPO_4$450.

(Figure 7, near here)

3.2.4. Activation parameters for the acrolein formation

The study of the rate of acrolein formation in the steady state at the three temperatures allows us to calculate the activation parameters (E_a and lnA) from the Arrhenius equation for all the solids studied, whose values are shown in Table 3. Despite a low number of data, a straight line, with values of correlation coefficients (r)

over 0.99 and significance levels higher than 91%, was obtained for the majority of the solids. The values of apparent E_a, ranging between 18 and 91 kJ/mol, were, in general, smaller than the scarce values reported in the literature and that have been obtained based on computational methods on homogeneous [33] and heterogeneous [32] catalysts. Furthermore, the relationship found between ln A and E_a, Figure 8, according to the equation, $\ln A = \ln\alpha + E_a/\theta R$, where θ is the isokinetic temperature at which identical values of reaction rate, α, are obtained, implies the existence of a "compensation effect" or "isokinetic relationship" [24]. This compensation effect would indicate a common interaction mechanism for glycerol dehydration to acrolein for all the solids studied. In this sense, at the three reaction temperatures, a relationship between the capacity of the solids to produce acrolein and the number of acid sites exhibited exists, as can be seen in Figure 9. In this Figure, the values of the rate of acrolein formation obtained at 250ºC in the steady state, shown in Table 3, against the acidity values in Table 1, are displayed. As a general tendency, the solids exhibiting a higher number of acid sites also showed higher values of acrolein formation rate, which is in accordance with that reported by several authors [16, 19, 20]. Therefore, the formation of acrolein on the catalysts here studied, would take place with the participation mainly of weak-medium acid sites, which are predominant according to the results of pyridine TPD. Such sites would be Lewis and Bronsted acids given that the pyridine is adsorbed on both types of acid sites. Furthermore, previous studies based on the analysis by DRIFT spectroscopy of desorbed pyridine in a temperature range between 50ºC and 300ºC, indicated that the $AlPO_4$ possesses both type of acid sites, the Lewis (Al^{3+}) being dominant over the Bronsted (P-OH) and also the strongest [26, 28].

(Table 3, Figure 8 and 9, near here)

However, the behaviour of the AlVPO(2)450 catalyst is noticeable, showing a superior capacity than expected to produce acrolein at temperatures above 220ºC, taking into account the acidity exhibited (Table 1). Therefore, we should assume that a higher number of acid sites, in addition to those evaluated by the pyridine TPD experiments, exist on this catalyst at temperatures superior than 220ºC. Such sites would be acid sites associated with the vanadyl group (V^{5+}=O) of the β-$VOPO_4$ phase, which also exhibits an oxidising character. In fact, a similar system to AlVPO(2)450, in which the β-$VOPO_4$ phase predominated over the $AlPO_4$ phase (molar ratio Al/V= 0.3), as well as an almost pure β-$VOPO_4$, were not able to retain pyridine, as we previously reported [24]. However, both solids presented activity in the 2-propanol dehydration, but at temperatures superior than AlVPO(2)450, their dehydration activity also being notably inferior. Moreover, the formation of new acid sites (V-OH) by addition of a water molecule (from aqueous glycerol feed or from the dehydration reaction) to a vanadyl group should not be ruled out. In fact, the presence of water in the feed brings about changes in the equilibrium between Lewis and Bronsted acid sites, favouring the formation of Bronsted sites [26].

On the other hand, the highest capacity of the binary systems containing V and Fe to also generate coke and unidentified compounds would be related to the highest percentage of strong acid sites that were exhibited, consequence of the interaction between the vanadium or iron species and those of aluminium, as aforementioned.

3.2.5. Possible reactions involved in the glycerol transformation

Based on the identified products in this study, the reactions involved in the glycerol transformation would be those shown in the Scheme 2. The initial dehydration glycerol would give the glycidol epoxide, whose opening gives hydroxyacetone and

mainly 3-hydroxypropanaldehyde because a secondary carbocation is implicated. This unstable aldehyde easily undergoes a dehydration forming the stable α-β-unsaturated aldehyde, propenaldehyde or acrolein. The 3-hydroxypropanaldehyde can also experiment other reactions, as a retro aldol condensation giving formaldehyde and acetaldehyde [9, 33, 34], although these compounds were not detected. However, the presence of acetaldehyde is generally reported not only in the glycerol transformation but also in that of hydroxyacetone [15, 17, 18, 35]. In addition to dehydration reactions, the glycerol can also undergo dehydrogenation reactions giving 2,3-dihydroxypropanaldehyde and 1,3-dihydroxypropanone, the formation of aldehyde being more probable due to the existence of two primary hydroxyl groups. These hydroxycarbonyl compounds would also decompose by a retro aldol condensation to glycolic aldehyde and formaldehyde, that could be oxidized to their respective acids, as have been detected in our study. In this sense, the formation of glycolic acid has been reported but carrying out the glycerol reaction in the presence of oxygen [36]. The formaldehyde formation as well as that of acetaldehyde in the present study could be demonstrated by the presence of compounds generated from subsequent reactions. Thus, in addition to formic acid the formaldehyde gave rise to cyclic acetals by reacting with glycerol, whereas acetaldehyde by hydrogenation produced ethanol, which reacts with glycolic acid to give ethyl glycolate. In fact, the highest values of yield to both reaction products, glycerol formal and ethyl glycolate, were attained with the solids exhibiting the highest yields to acrolein. Furthermore, we suggest that glycolic acid and acetaldehyde could also undergo a polymerization, explaining the low percentage or the absence of these compounds in the catalysts, in which the percentage of "others" compounds was more relevant, Figure 7, given that in these compounds could be included the polymerization products.

(Scheme 2, near here)

4. Conclusions

In the present experimental conditions (0.6 mL/min of 36 wt% glycerol aqueous solution; 100 mg of catalyst and reaction temperatures of 220ºC, 250ºC and 280ºC), the main product in the transformation of glycerol was acrolein with all the phosphates studied. Other products such as hydroxyacetone, glycidol, glycerol formal, glycolic acid, diglycerol and ethyl glycolate were also detected.

The catalysts presented good stability, they did not suffer deactivation after more than 14 h of reaction. The amorphous $FePO_4$ and $AlPO_4$ exhibited a higher yield to acrolein than the other simple phosphates, which possess a high crystalline character. However, the modification of aluminium phosphate with Fe (by co-precipitation or impregnation) and V, even in small quantities, gave rise to more active and selective catalysts to produce acrolein, whereas the presence of Ca did not promote its activity. Thus, the aluminum-vanadium phosphate (molar ratio Al/V=2) showed the highest value of yield to acrolein, 62% (equivalent to a productivity of 0.88 $\frac{g_{ACR}}{g_{cat} \cdot h}$) at 280ºC, which was similar to those values reported in literature. It is worth mentioning that, in the gas-phase the acrolein productivity was appreciably superior than in liquid phase.

A common interaction mechanism for glycerol dehydration to acrolein for all the solids studied could be considered, due to the existence of a linear relationship between the values of ln A and E_a (ranging between 18 and 91 kJ/mol). Such a mechanism would imply the participation mainly of the acid sites, specifically acid sites (POH; Al^{3+}) of weak-medium strength that were predominant, although the participation of acid sites with redox properties (like V^{5+}=O) may also be taken into account, especially at temperatures higher than 220ºC. Indeed, the strong acid sites favoured secondary

reactions of glycerol as well as acrolein and other dehydration products, giving coke mainly at the beginning of the reaction, and unidentified compounds in the steady state. The binary phosphates with V and Fe also exhibiting the highest percentage and density of strong acid sites, promoted those reactions.

Based on the identified products in this study, some possible reactions involved in the glycerol transformation have been suggested. Thus, the dehydration reactions giving 3-hydroxypropanaldehyde (acrolein precursor) and hydroxyacetone, would start with the formation of glycidol epoxide.

Acknowledgements

Subsidies granted by the Ministerio de Educación y Ciencia and FEDER funds (Project CTQ2010-18126, ENE2011-27017) and Junta de Andalucía and FEDER funds (P11-TEP-7723) are gratefully acknowledged. S. Lopez-Pedrajas is indebted to the Ministerio de Educación, Ciencia y Deporte for a FPU fellowship.

References

[1] OECD-FAO Agricultural Outlook 2013-2022.

[2] Z. Gholami, A.Z. Abdullah, K.-T. Lee, Renew. Sust. Energ. Rev. 39 (2014) 327-341.

[3] C.H. Zhou, H. Zhao, D.S. Tong, L.M. Wu, W.H. Yu, Catal. Rev.-Sci. Eng. 55 (2013) 369-453.

[4] M. Pagliaro, R. Ciriminna, H. Kimura, M. Rossi, C. Della Pina, Angew. Chem. Int. Edit. 46 (2007) 4434-4440.

[5] A. Corma, S. Iborra, A. Velty, Chem. Rev. 107 (2007) 2411-2502.

[6] A. Talebian-Kiakalaieh, N.A.S. Amin, H. Hezaveh, Renew. Sust. Energ. Rev. 40 (2014) 28-59.

[7] B. Katryniok, S. Paul, F. Dumeignil, ACS Catal. 3 (2013) 1819-1834.

[8] J.L. Dubois, C. Duquenne, W.H. Hoelderich, J. Kervennal, to Arkema, FR2882053 (2005).

[9] S.-H. Chai, H.-P. Wang, Y. Liang, B.-Q. Xu, Green Chem. 9 (2007) 1130-1136.

[10] P. Lauriol-Garbey, S. Loridant, V. Bellière-Baca, P. Rey, J.-M.M. Millet, Catal. Commun. 16 (2011) 170-174.

[11] Y.T. Kim, K.-D. Jung, E.D. Park, Micropor. Mesopor. Mat. 131 (2010) 28-36.

[12] Y.T. Kim, K.-D. Jung, E.D. Park, Appl. Catal. A-Gen. 393 (2011) 275-287.

[13] Z. Wang, L. Wang, Y. Jiang, M. Hunger, J. Huang, ACS Catal. 4 (2014) 1144-1147.

[14] A. Alhanash, E.F. Kozhevnikova, I.V. Kozhevnikov, Appl. Catal. A-Gen. 378 (2010) 11-18.

[15] W. Suprun, M. Lutecki, T. Haber, H. Papp, J. Mol. Catal. A-Chem. 309 (2009) 71-78.

[16] W. Suprun, M. Lutecki, H. Papp, Chem. Eng. Technol. 34 (2011) 134-139.

[17] J. Deleplanque, J.-L. Dubois, J.-F. Devaux, W. Ueda, Catal. Today 157 (2010) 351-358.

[18] F. Wang, J.-L. Dubois, W. Ueda, J. Catal. 268 (2009) 260-267.

[19] N.P. Rajan, G.S. Rao, B. Putrakumar, K.V. Chary, RSC Adv. 4 (2014) 53419-53428.

[20] C.S. Carriço, F.T. Cruz, M.B. Santos, H.O. Pastore, H.M.C. Andrade, A.J.S. Mascarenhas, Micropor. Mesopor. Mat. 181 (2013) 74-82.

[21] J.M. Campelo, A. Garcia, D. Luna, J.M. Marinas, J. Catal. 111 (1988) 106-119.

[22] J.M. Campelo, J.M. Marinas, S. Mendioroz, J.A. Pajares, J. Catal. 101 (1986) 484-495.

[23] R. Navarro, S. Lopez-Pedrajas, D. Luna, J.M. Marinas, F.M. Bautista, Appl. Catal. A-Gen. 474 (2014) 272-279.

[24] F.M. Bautista, J.M. Campelo, A. García, D. Luna, J.M. Marinas, A.A. Romero, M.T. Siles, Catal. Today 78 (2003) 269-280.

[25] F.M. Bautista, J.M. Campelo, A. Garcıa, D. Luna, J.M. Marinas, R.A. Quiros, A.A. Romero, Appl. Catal. A-Gen. 243 (2003) 93-107.

[26] F.M. Bautista, B. Delmon, Appl. Catal. A-Gen. 130 (1995) 47-65.

[27] J.M. Campelo, A. Garcia, J.F. Herencia, D. Luna, J.M. Marinas, A.A. Romero, J. Catal. 151 (1995) 307-314.

[28] R. Estevez, S. Lopez-Pedrajas, F. Blanco-Bonilla, D. Luna, F.M. Bautista, Chem. Eng. J. 282 (2015) 179-186.

[29] N.P. Rajan, G.S. Rao, V. Pavankumar, K.V. Chary, Catal. Sci. Technol. 4 (2014) 81-92.

[30] S.Y. Liu, C.J. Zhou, Q. Liu, G.C. Liu, C.J. Huang, Z.S. Chao, ChemSusChem 1 (2008) 575-578.

[31] J.L. Dubois, to Arkema, WO2010046227 (2010).

[32] K. Kongpatpanich, T. Nanok, B. Boekfa, M. Probst, J. Limtrakul, Phys. Chem. Chem. Phys. 13 (2011) 6462-6470.

[33] M.R. Nimlos, S.J. Blanksby, X. Qian, M.E. Himmel, D.K. Johnson, J. Phys. Chem. A 110 (2006) 6145-6156.

[34] E. Tsukuda, S. Sato, R. Takahashi, T. Sodesawa, Catal. Commun. 8 (2007) 1349-1353.

[35] A. Corma, G.W. Huber, L. Sauvanaud, P. O'Connor, J. Catal. 257 (2008) 163-171.

[36] B. Katryniok, H. Kimura, E. Skrzyńska, J.-S. Girardon, P. Fongarland, M. Capron, R. Ducoulombier, N. Mimura, S. Paul, F. Dumeignil, Green Chem. 13 (2011) 1960-1979.

Figure

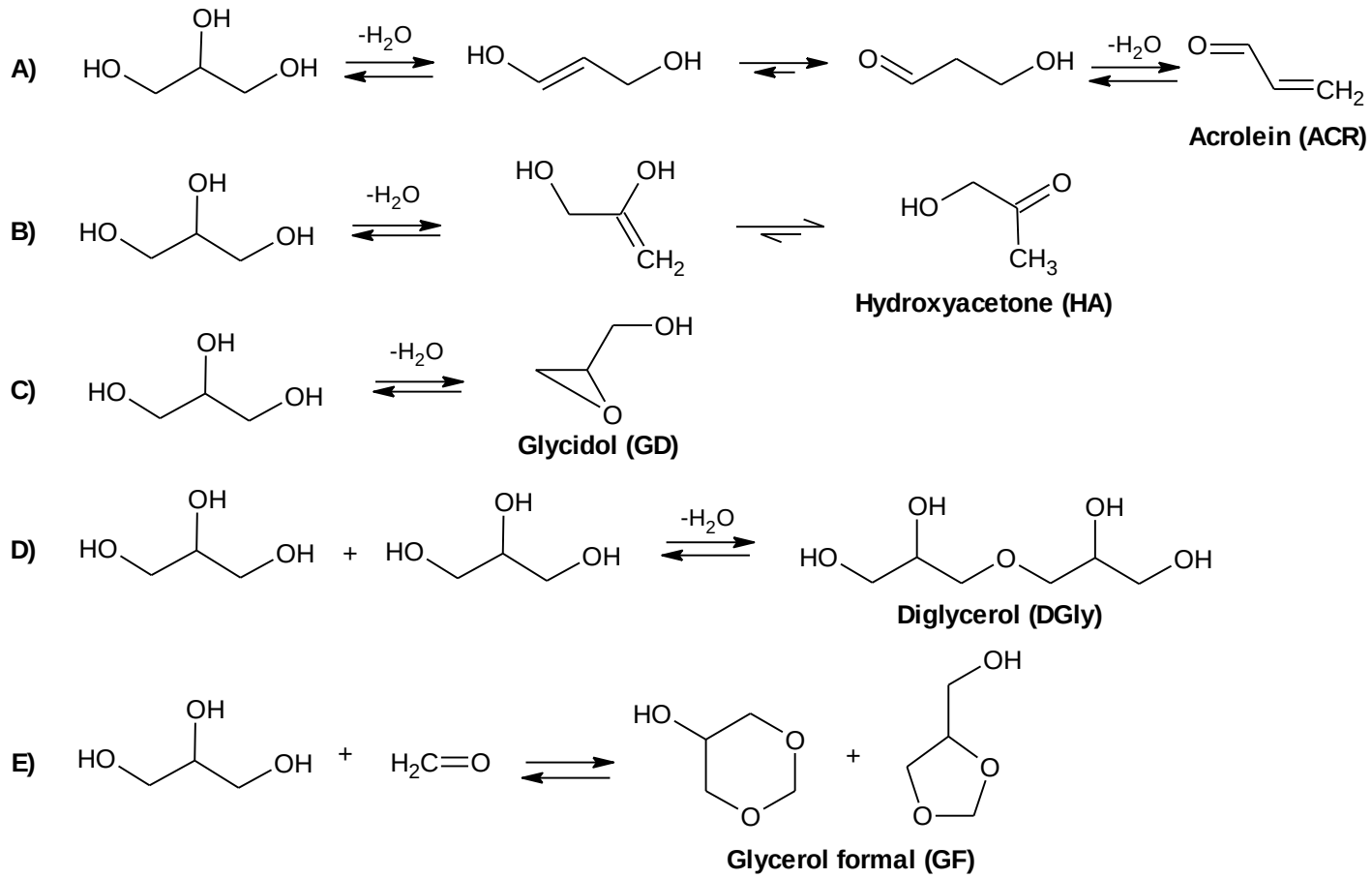

Scheme 1

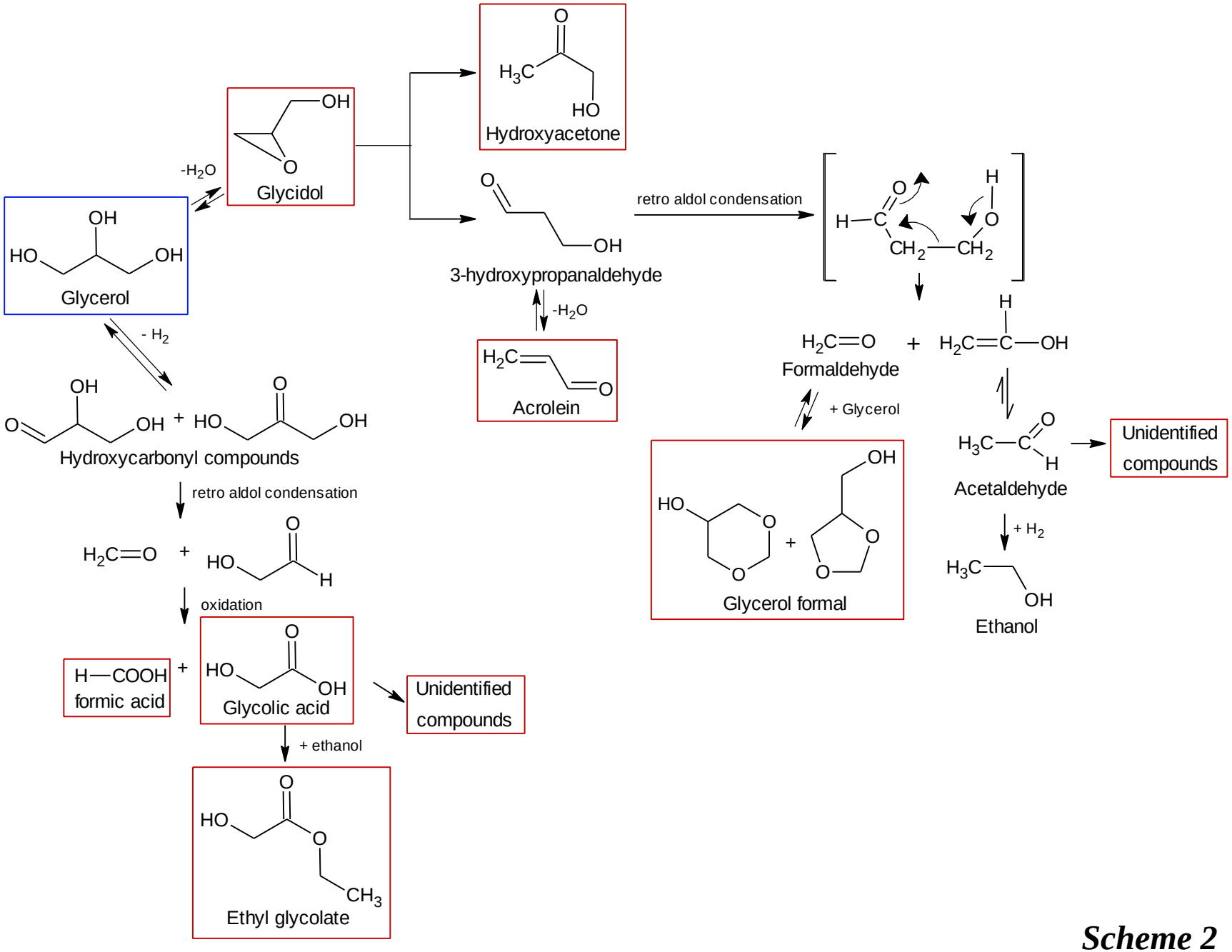
Hydroxyacetone
Glycidol
-H2O
Glycerol
3-hydroxypropanaldehyde
retro aldol condensation
- H2
-H2O
Acrolein
Hydroxycarbonyl compounds
retro aldol condensation
Formaldehyde
+ Glycerol
Glycerol formal
Acetaldehyde
Unidentified compounds
oxidation
+ H2
Ethanol
H—COOH formic acid
Glycolic acid
Unidentified compounds
+ ethanol
Ethyl glycolate

Scheme 2

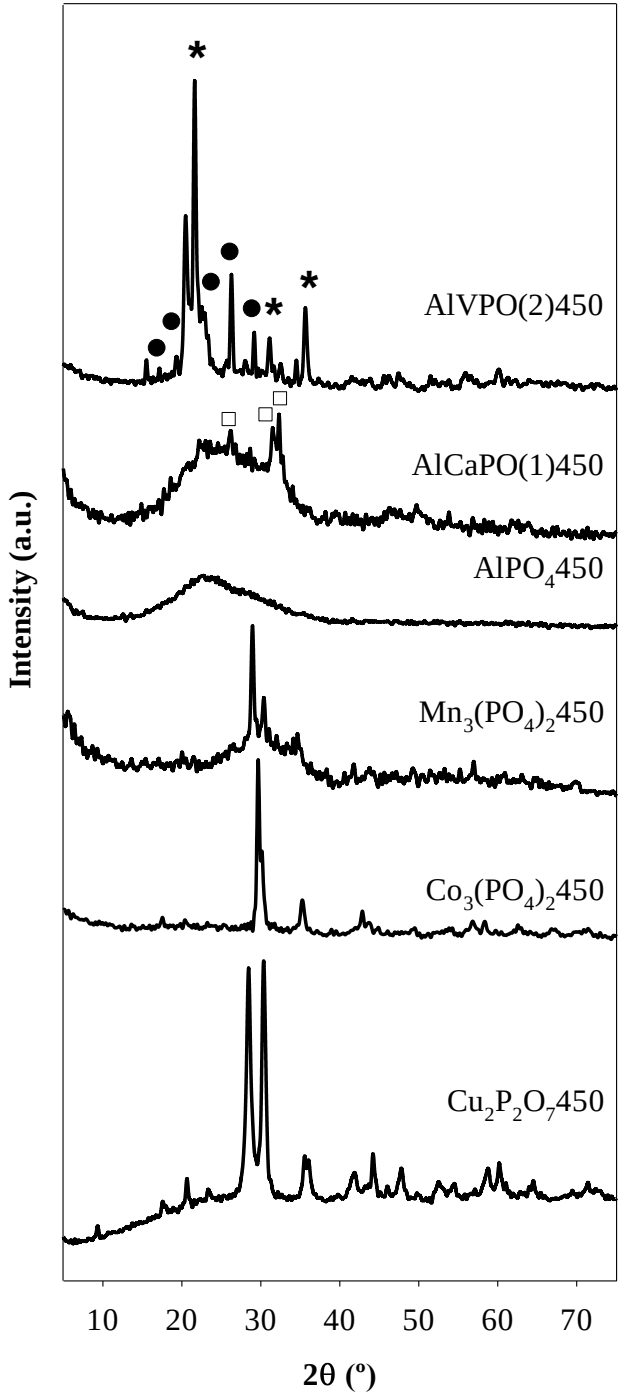
Intensity (a.u.)
AlVPO(2)450
AlCaPO(1)450
AlPO4450
Mn3(PO4)2450
Co3(PO4)2450
Cu2P2O7450
10
20
30
40
50
60
70
2θ (º)

Figure 1

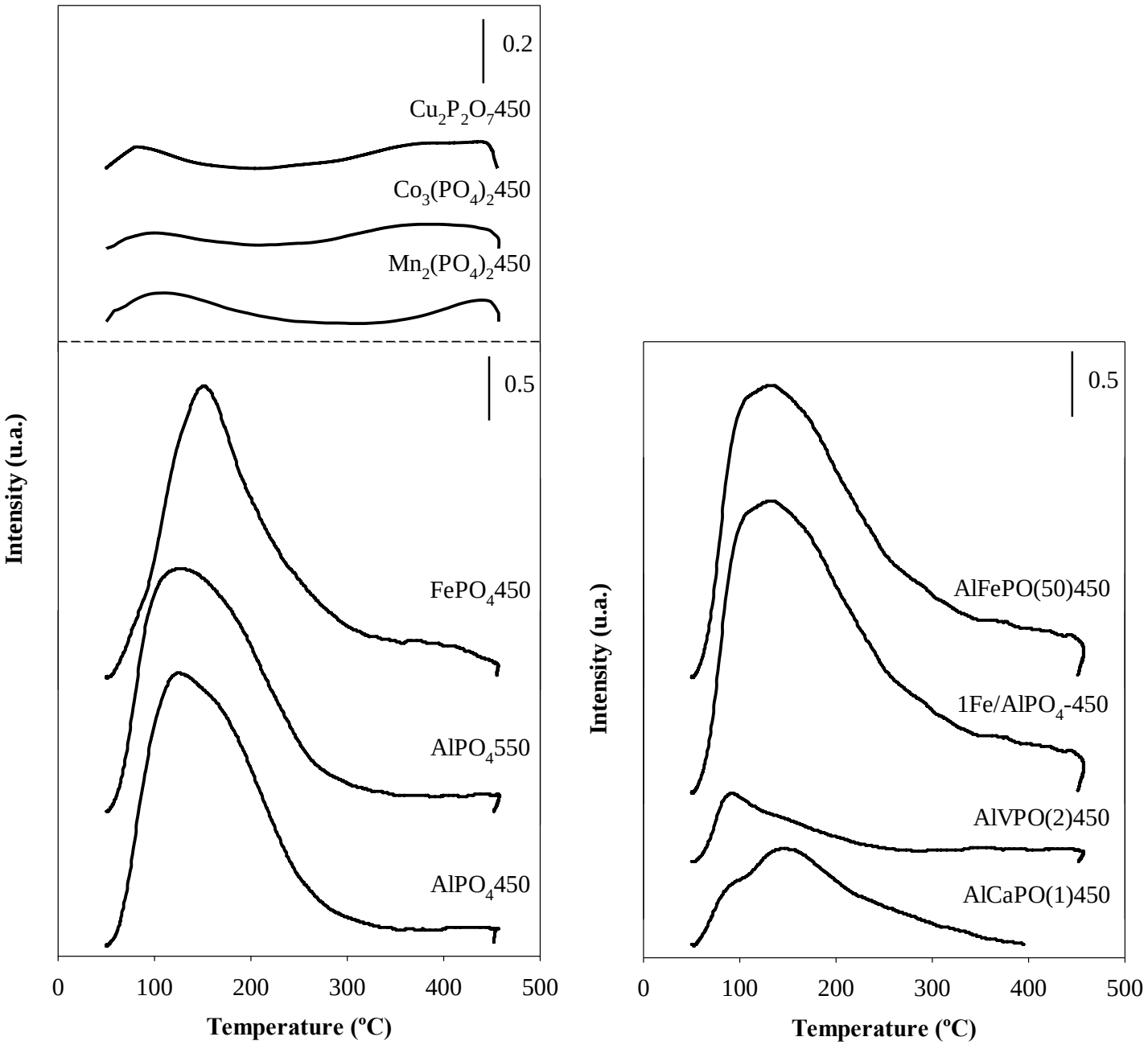
0.2
$Cu_2P_2O_7$450
$Co_3(PO_4)_2$450
$Mn_2(PO_4)_2$450
0.5
$FePO_4$450
$AlPO_4$550
$AlPO_4$450
Intensity (u.a.)
0
100
200
300
400
500
Temperature (ºC)
0.5
AlFePO(50)450
1Fe/$AlPO_4$-450
AlVPO(2)450
AlCaPO(1)450
Intensity (u.a.)
0
100
200
300
400
500
Temperature (ºC)

Figure 2

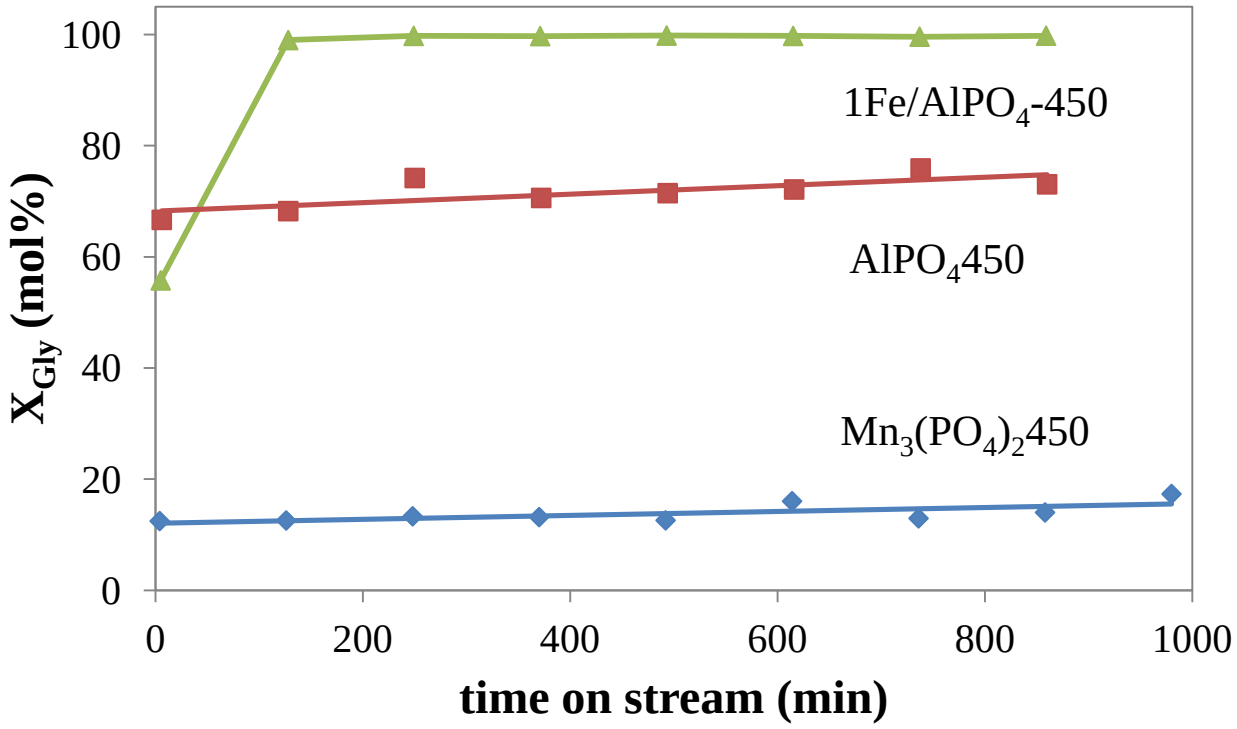
100
80
60
40
20
0
0
200
400
600
800
1000
X_{Gly} (mol%)
time on stream (min)
1Fe/AlPO$_4$-450
AlPO$_4$450
Mn$_3$(PO$_4$)$_2$450

Figure 3

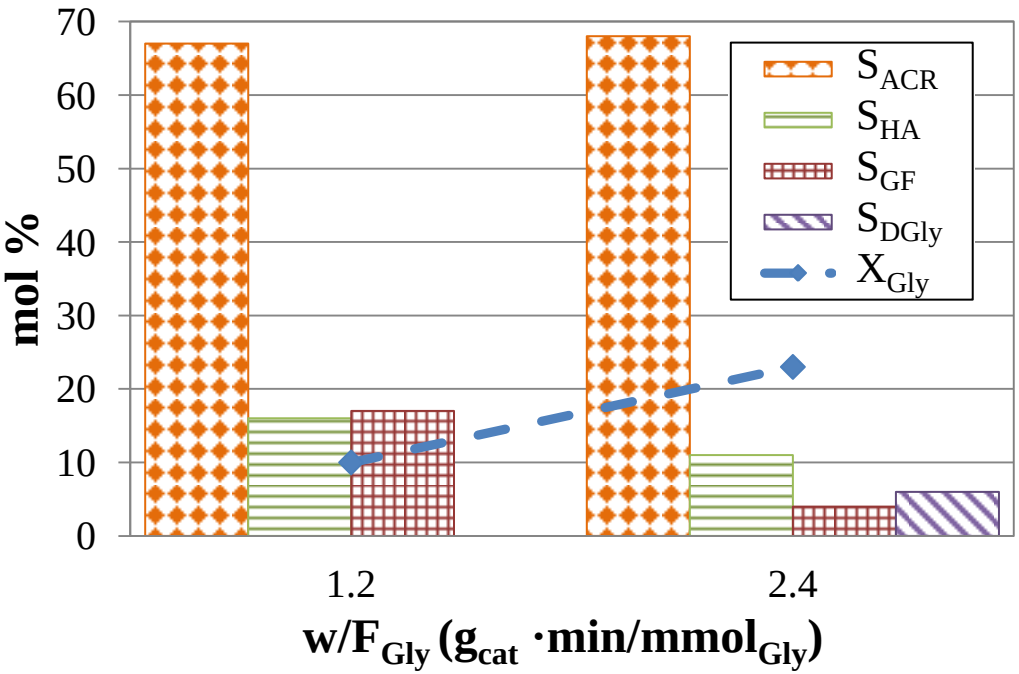
70
60
50
40
30
20
10
0
mol %
1.2
2.4
w/F Gly (g cat ·min/mmol Gly)
S ACR
S HA
S GF
S DGly
X Gly

Figure 4

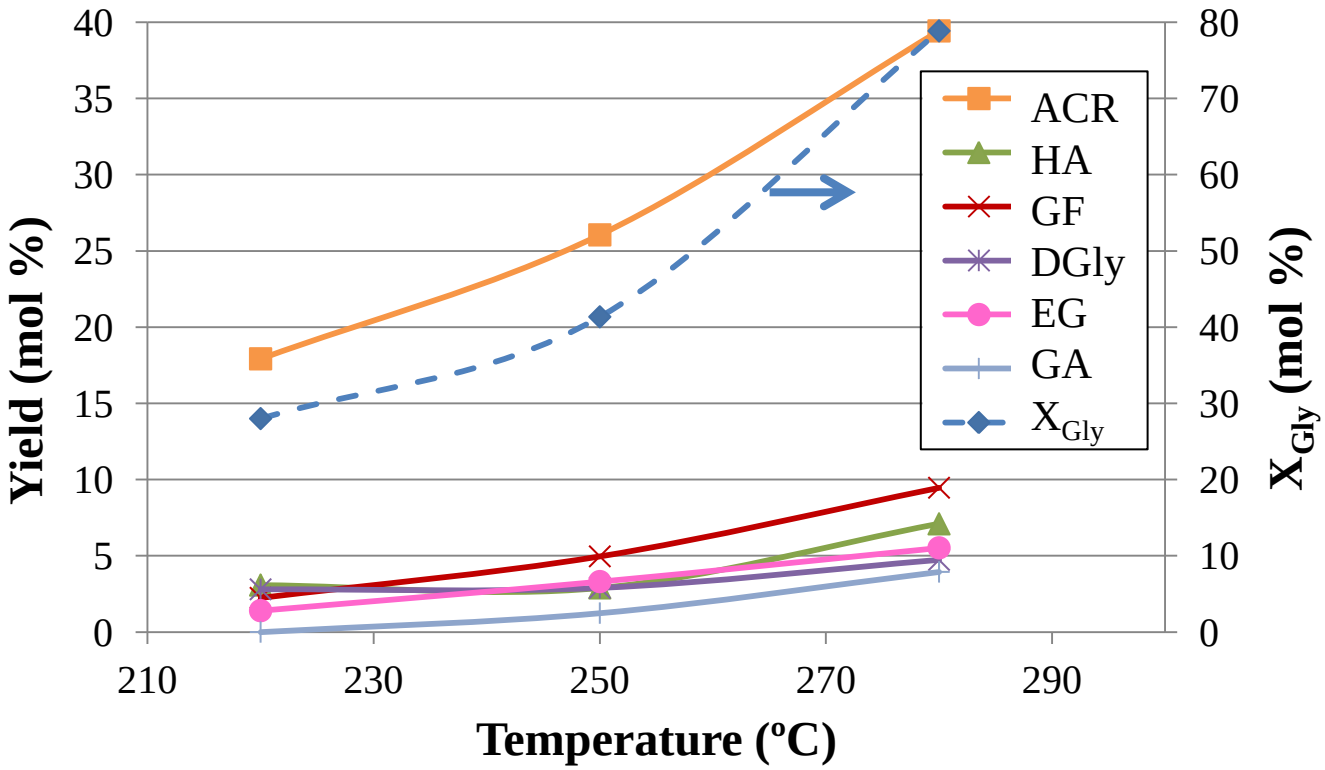
40
35
30
25
20
15
10
5
0
80
70
60
50
40
30
20
10
0
210
230
250
270
290
Yield (mol %)
X_Gly (mol %)
Temperature (ºC)
ACR
HA
GF
DGly
EG
GA
X_Gly

Figure 5

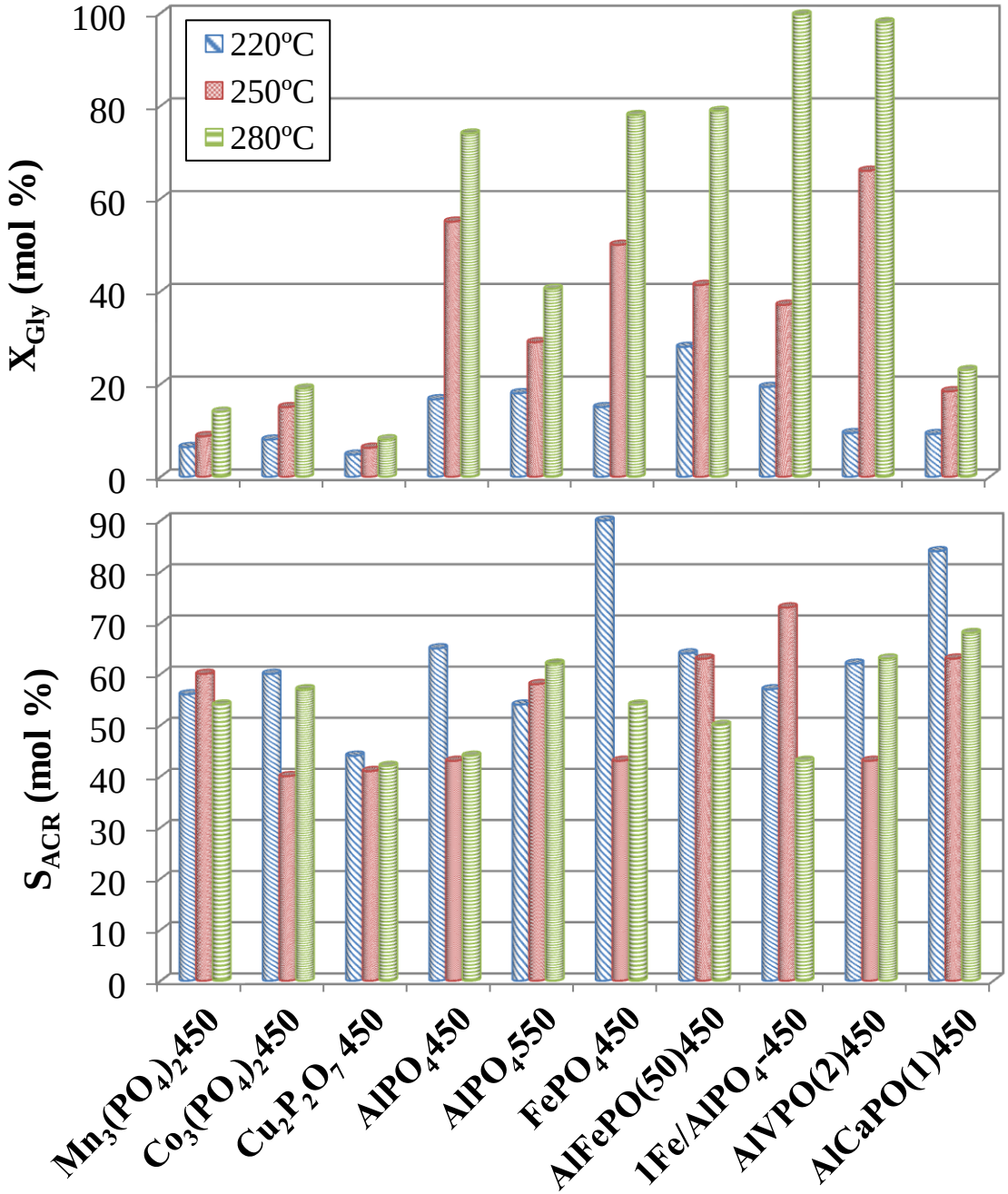
220ºC
250ºC
280ºC
X_{Gly} (mol %)
S_{ACR} (mol %)
100
80
60
40
20
0
90
70
50
30
10
$Mn_3(PO_4)_2$450
$Co_3(PO_4)_2$450
$Cu_2P_2O_7$ 450
$AlPO_4$450
$AlPO_4$550
$FePO_4$450
AlFePO(50)450
1Fe/$AlPO_4$-450
AlVPO(2)450
AlCaPO(1)450

Figure 6

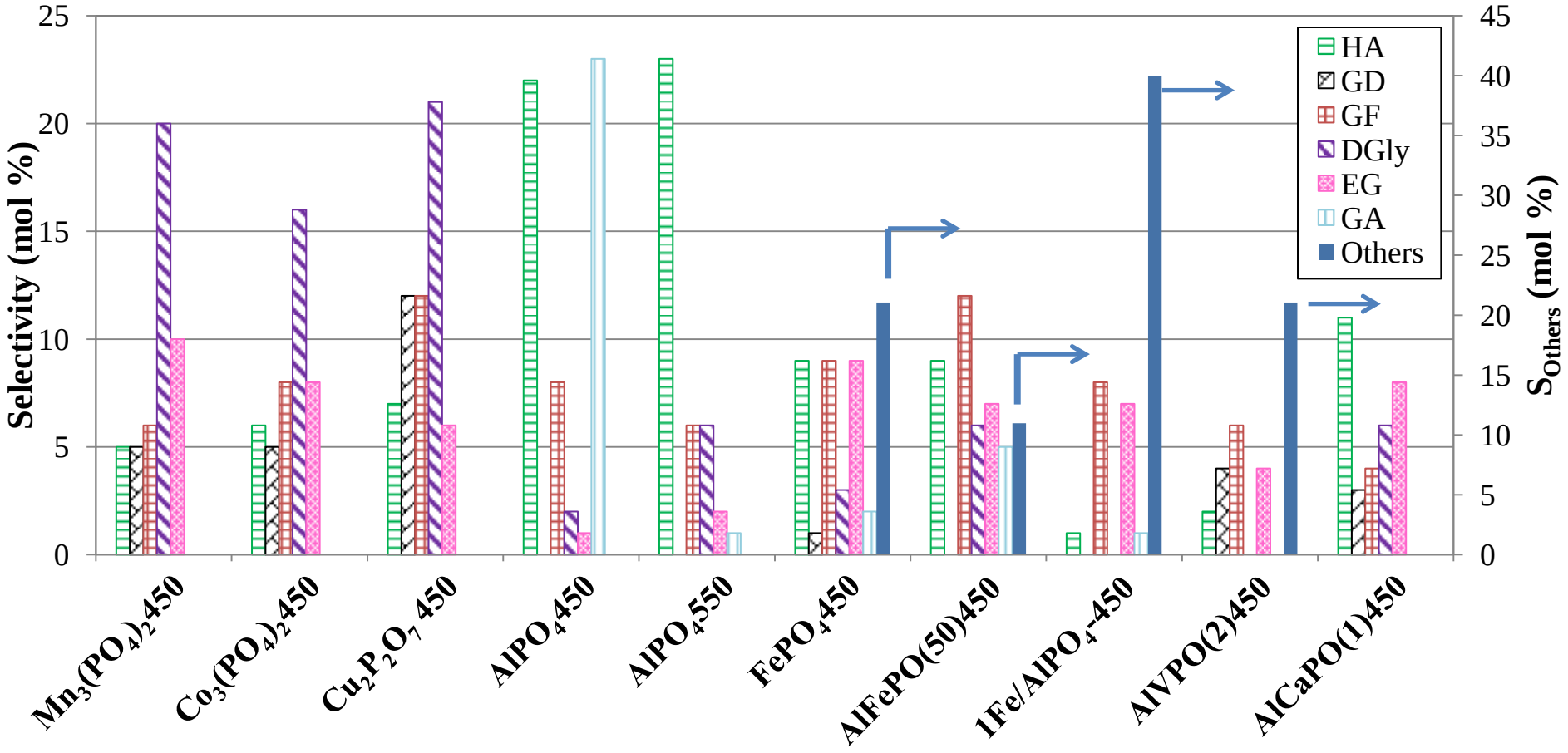
Selectivity (mol %)
S_{Others} (mol %)
HA
GD
GF
DGly
EG
GA
Others
$Mn_3(PO_4)_2$450
$Co_3(PO_4)_2$450
$Cu_2P_2O_7$ 450
$AlPO_4$450
$AlPO_4$550
$FePO_4$450
AlFePO(50)450
1Fe/$AlPO_4$-450
AlVPO(2)450
AlCaPO(1)450

Figure 7

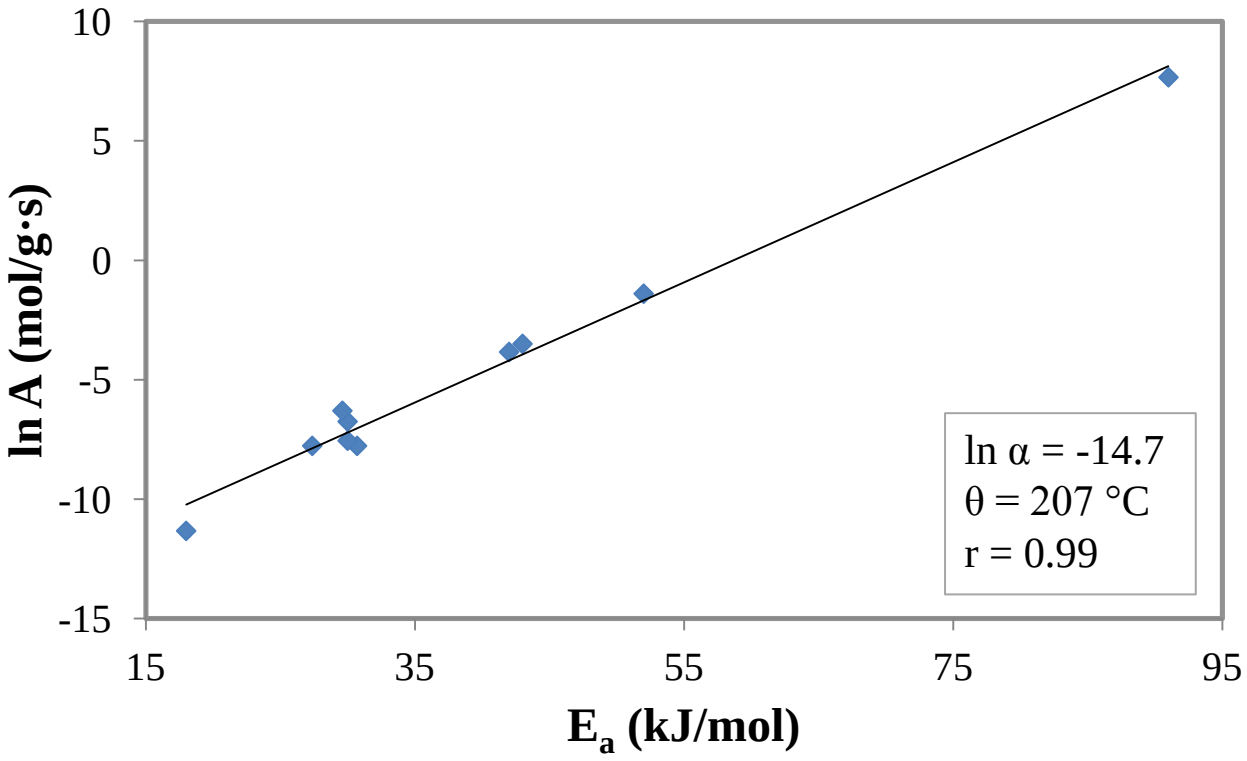

Figure 8

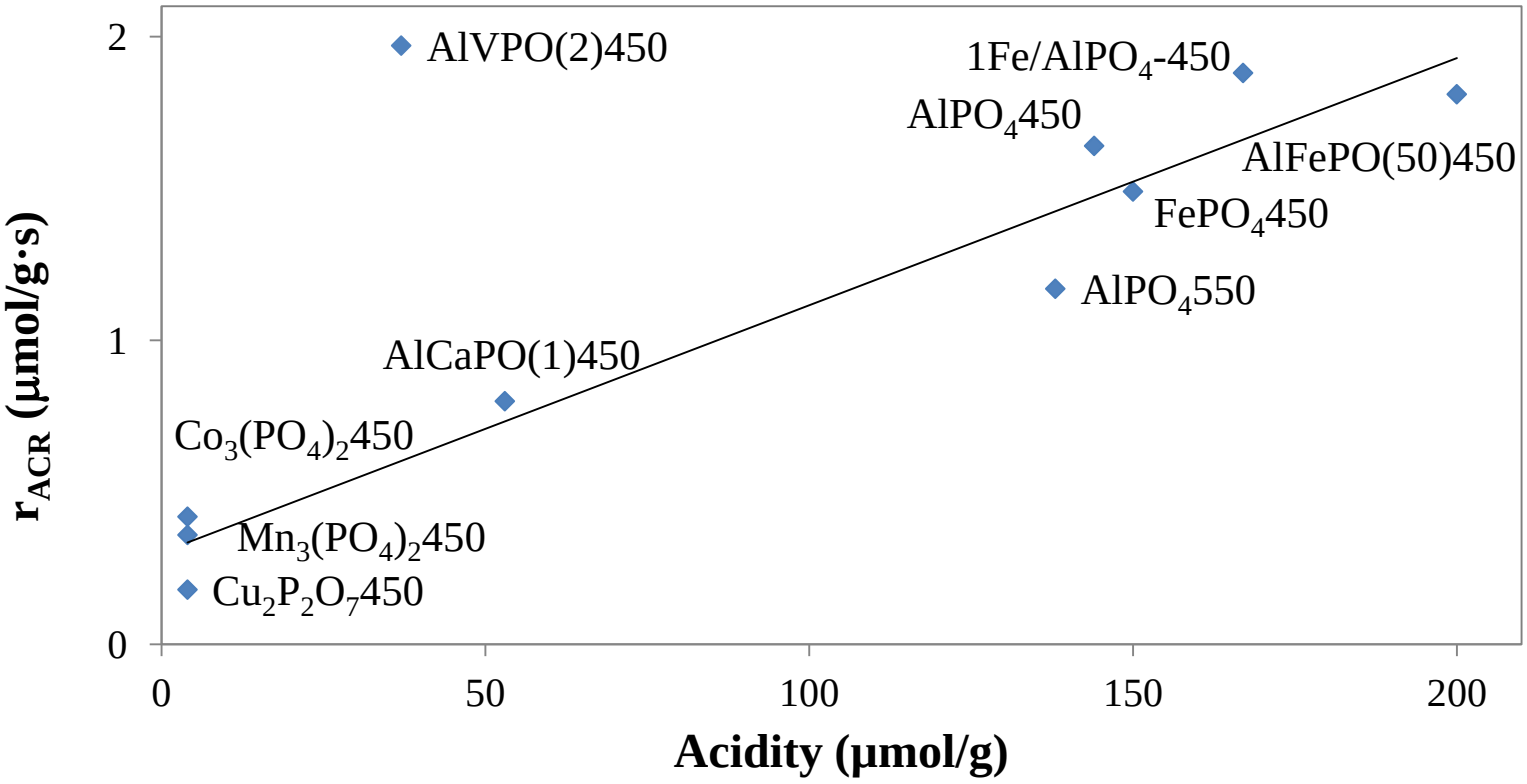
2
1
0
0
50
100
150
200
r_{ACR} (µmol/g·s)
Acidity (µmol/g)
AlVPO(2)450
1Fe/AlPO$_4$-450
AlPO$_4$450
AlFePO(50)450
FePO$_4$450
AlPO$_4$550
AlCaPO(1)450
Co$_3$(PO$_4$)$_2$450
Mn$_3$(PO$_4$)$_2$450
Cu$_2$P$_2$O$_7$450

Figure 9

Scheme Legends

Scheme 1. Reaction products obtained in the glycerol transformation: A) Acrolein, B) Hydroxyacetone, C) Glycidol, D) Diglycerol, E) Glycerol formal

Scheme 2. Possible reactions involved in the glycerol transformation. The detected products are shown by rectangles.

Figure Legends

Figure 1. XRD patterns of all the solids studied (● β-$VOPO_4$; *$AlPO_4$, α-cristobalite; □ CaP_2O_6).

Figure 2. Pyridine-TPD profiles of all the solids studied.

Figure 3. Conversion of glycerol as a function of time on stream. (36 wt% glycerol; F_{Gly}= 0.69 μmol/s; F_{N_2}= 75mL/min; w= 0.1g; T=280°C).

Figure 4. Values of glycerol conversion and selectivity to products at different contact times over AlCaPO(1)450 obtained in the steady state. (36 wt% glycerol; F_{Gly}= 0.69 μmol/s; F_{N_2}= 75mL/min; T=280°C).

Figure 5. Values of glycerol conversion and yield to reaction products as a function of reaction temperature in the steady state. Catalyst: AlFePO(50)450. (36 wt% glycerol; F_{Gly}= 0.69 μmol/s; F_{N_2}= 75mL/min; w= 0.1g).

Figure 6. Values of glycerol conversion and selectivity to acrolein as a function of reaction temperature in the steady state on all the catalysts. (Experimental conditions as in Figure 5).

Figure 7. Values of yield to reaction products at 280ºC in the steady state on all the catalysts. (Experimental conditions as in Figure 5).

Figure 8. Compensation effect between the activation parameters (ln A and E_a) collected in Table 2.

Figure 9. Influence of acidity of the catalysts (Table 1) on the rate of acrolein formation obtained at 250ºC (Table 3).

Table 1. Textural properties and acidity measurements from Py-TPD on all the solids studied.

Catalyst	S_{BET} (m^2/g)	V_p (mL/g)	d_p (Å)	Pore size distribution (%)		Acidity		Strength of acid sites (%)		
				> 500 Å	500-20 Å	(µmol/g)	(µmol/m^2)	Weak (80-200ºC)	Medium (200-300ºC)	Strong (>300ºC)
$Mn_3(PO_4)_2$450	16.8 ± 0.1	0.09	204	76	24	4	0.2	-	-	-
$Co_3(PO_4)_2$450	8.2 ± 0.1	0.06	290	57	43	4	0.5	-	-	-
$Cu_2P_2O_7$450	10.71 ± 0.08	0.06	220	60	40	4	0.4	-	-	-
$AlPO_4$450	217.6 ± 0.8	0.96	177	11	88	144	0.7	72	20	8
$AlPO_4$550	221 ± 1	0.96	174	11	88	138	0.6	71	21	8
$FePO_4$450	55.8 ± 0.1	0.31	223	25	75	150	2.7	63	25	12
AlFePO(50)450	248 ± 1	1.04	168	17	82	200	0.8	60	25	15
1Fe/$AlPO_4$-450	218.5 ± 0.7	0.99	181	8	91	167	0.8	64	23	13
AlVPO(2)450	23.3 ± 0.2	0.10	169	68	32	37	1.6	64	16	20
AlCaPO(1)450	52.6 ± 0.1	0.26	195	60	39	53	1.0	67	27	6

Table 2. Values of acrolein productivity obtained on the most active solids here investigated and on several phosphates reported in the literature.

Catalyst	Temperature (ºC)	Acrolein productivity (g_{acr}/g_{cat}·h)	Reference
$AlPO_4$450	280	0.46	This manuscript
$AlPO_4$450** \| **$AlPO_4$650	270 (liquid phase)	0.07 | 0.17	[28]
PO_4/Al_2O_3	280	0.04	[15]
1Fe/$AlPO_4$-450	280	0.61	This manuscript
$Fe_x(PO_4)_y$	280	0.13	[17]
AlVPO(2)450	280	0.88	This manuscript
VPO	280	0.17	[31]
$VOHPO_4 \cdot 0.5H_2O$	300 (with O_2)	0.20	[18]
VPO (P/V =2)	300 (with O_2)	0.20	[19]
20wt%VPO/ZrP	300	0.18	[29]
$WOx/Al_2O_3/PO_4$	265	0.10[a]	[16]
Meso-LaCuCrAlPO	340	7.54[b]	[30]

[a]assuming that w= 0.2 g, as in a previous publication by Suprun et al. [15]
[b]assuming that the reagent was pure glycerol.

Table 3. Values of acrolein formation rate (r_{ACR}) obtained in the steady state on all the catalysts and temperatures studied, at the same experimental conditions as in Figure 5, as well as the corresponding activation parameters (E_a and ln A).

Catalysts	Temperature (ºC)	r_{ACR} (μmol/g·s)	E_a (kJ/mol)	ln A (mol/g·s)	r*	Significance (%)
$Mn_3(PO_4)_2$450	220	0.25	31	-7.77	0.999	96
	250	0.36				
	280	0.52				
$Co_3(PO_4)_2$450	220	0.33	30	-7.55	0.959	82
	250	0.42				
	280	0.75				
$Cu_2P_2O_4$450	220	0.14	18	-11.34	0.992	92
	250	0.18				
	280	0.23				
$AlPO_4$450	220	0.75	42	-3.84	0.979	87
	250	1.64				
	280	2.26				
$AlPO_4$550	220	0.67	30	-6.75	0.999	98
	250	1.17				
	280	1.74				
$FePO_4$450	220	0.94	43	-3.49	0.991	91
	250	1.45				
	280	2.92				
AlFePO(50)450	220	1.24	30	-6.35	0.999	96
	250	1.81				
	280	2.73				
1Fe/$AlPO_4$-450	220	0.76	52	-1.40	0.988	90
	250	1.88				
	280	2.97				
AlVPO(2)450	220	0.40	91	7.66	0.991	91
	250	1.97				
	280	4.28				
AlCaPO(1)450	220	0.54	27	-7.77	1	98
	250	0.80				
	280	1.08				

*regression coefficients